2025 IEEE XVII International Scientific and Technical Conference on Actual Problems of Electronic Instrument Engineering (APEIE) | 979-8-3315-5916-8/25/$31.00 ©2025 IEEE | DOI: 10.1109/APEIE66761.2025.11289407

Proceedings of the

XVII International Scientific and Technical Conference «Actual Problems of Electronic Instrument Engineering»

APEIE

APEIE25
Actual Problems of Electronic Instrument Engineering

14–16 November 2025, Russia

IEEE Catalog Number: CFP25471-ART
ISBN: 979-8-3315-5916-8

2025 IEEE XVII International Scientific and Technical Conference on Actual Problems of Electronic Instrument Engineering (APEIE) | 979-8-3315-5916-8/25/$31.00 ©2025 IEEE | DOI: 10.1109/APEIE66761.2025.11289252

IEEE Catalog Number: CFP25471-ART
ISBN: 979-8-3315-5916-8

2025 IEEE XVII International Scientific and Technical Conference on Actual Problems of Electronic Instrument Engineering (APEIE) | 979-8-3315-5916-8/25/$31.00 ©2025 IEEE | DOI: 10.1109/APEIE66761.2025.11289382

Detection of Layer-like Conducting Objects Based on Electromagnetic Sensing Signals Using Three-dimensional Mathematical Modeling

Nadezhda V. Shtabel
Laboratory of mathematical modeling of multiphase processes in native and artificial *multiscale heterogeneous media*
Trofimuk Institute of Petroleum Geology and Geophysics, SBRAS
dept. of Geophysical Systems
Novosibirsk State Technical University
Novosibirsk, Russia
0000-0003-0390-9298

***Abstract*— The paper considers the problem of identifying the relationship between the parameters of a conductive object and EMF signals. Models of a localized object in a half-space and an object covered by a conductive layer are investigated. As a result of three-dimensional mathematical modeling, EMF signals in time are obtained for various models of the environment and the position of the object. The distributions of abnormal signals according to the calculated EMF are constructed. A method for estimating the parameters of an object based on the revealed dependencies of abnormal signals on the position of the object and its induction mass is proposed. The characteristic dependences applicable for rapid assessment of body parameters without three-dimensional inversion are revealed. The results demonstrate the possibility of estimating the depth of the upper edge of the target object and its induction mass by measuring anomalies in EMF signals. However, to improve the accuracy of estimates, it is necessary to take into account the time required for the field to propagate in the upper layer.**

Keywords*— *electrical exploration, numerical modeling, finite element method, inversion, conductive object

I. INTRODUCTION

Interpretation of electromagnetic sounding data is based on the analysis of induced EMF signals, a priori information about the geology of the studied area, and the use of specialized inversion programs[1], [2]. Modern algorithms, such as the conjugate gradient method, genetic algorithms, or Monte Carlo methods, make it possible to minimize the functional deviations between the measured data and the calculated EMF signals obtained for a given medium model [3]. For example, popular software packages (EMIGMA, ModEM, and AarhusInv) use hybrid approaches that combine Tikhonov regularization and stochastic optimization, which increases the stability of the solution in noisy data conditions. An important step is to take into account a priori data: lithological sections of wells, seismic survey results, or petrophysical properties of rocks, which set the initial constraints for modeling [4].

Three-dimensional Bayesian inversions are a powerful tool for solving geophysical inverse problems, allowing us to take into account not only measurement uncertainties, but also correlations between various environmental parameters, such as electrical conductivity, porosity, and mineral composition [5]. Unlike deterministic methods, the Bayesian approach relies on a posteriori probability distribution, which makes it possible to evaluate the reliability of the obtained models. For example, works [6], [7] demonstrate how the integration of magnetotelluric and seismic data within the Bayesian approach makes it possible to reconstruct complex subduction zones with an accuracy of up to 10% in terms of conductivity. However, despite the reliability of the results, the method requires significant computational resources, especially when working with highly detailed grids, where the number of unknown parameters can reach millions.

The solution of the inverse problem is usually aimed at specifying one group of parameters: the geometric dimensions of the body (for example, reservoir thickness), its position in space (depth of occurrence, tilt angles), or the physical properties of the object (resistivity, anisotropy). Multi-stage inversion may be required to reconstruct a model of an environment with a complex three-dimensional structure, such as salt domes or fault zones. At the first stage, a quasi-two-dimensional approximation is often used to roughly determine the contours of the anomaly, then full-size 3D algorithms are employed. Each iteration of refining the initial model takes from several hours to a day, depending on the speed of solving a direct problem (for example, the finite element method on GPU clusters speeds up calculations by 50-100 times) and the number of parameters. Current trends include the use of neural network emulators for direct problems, which reduces iteration time by 40-60%, as shown in studies [8].

In this paper, the effect of various parameters of a conducting body in a weakly conducting space on anomalous EMF signals is studied in order to identify characteristic dependencies that could be used for rapid estimation of body parameters without performing a three-dimensional inversion.

II. METHODS

Let us consider a model of a medium containing a layer-like conducting body in a weakly conducting space. The size of the object is 300x200x10 m, the depth of the upper edge varies from 40 to 190 m in increments of 50 m. The resistance of the host medium is 500-1200 ohm·m. The resistance of the host medium was set to 1000·ohm·m by default. The electrical conductivity of the object varied from 0.1 Cm/m to 0.2 Cm/m. In the model with an object covered

by a near surface layer, the thickness of the layer varied from 40 to 80 m with a resistance of 50 ohm·m.

The probe setup is represented by a generator loop with a side of 500 m and 49 receiving loops with a side of 100 m, located over the area inside the generator loop with a step of 50 m between the it`s centers. Such a dense network of observations makes it possible to determine the position of a local object and its boundaries at small depths from the EMF distribution over the area at a fixed time.

Conductive objects result in increased EMF values, the maximum of which in the area distribution is located in the projection of the object's center. The position of the maximum in the plan is preserved for the entire measurement time from the moment of occurrence of secondary eddy currents in the object until their disappearance.

III. MATHEMATICAL MODEL

The electromagnetic field is governed by the Maxwell's system of equations:

$$\begin{cases} \dfrac{\partial \vec{B}}{\partial t} = -curl\vec{E}, \\ \dfrac{\partial \vec{D}}{\partial t} = curl\vec{H} - \sigma\vec{E} - \vec{J}, \end{cases}$$
$$div\vec{B} = 0, \quad div\vec{D} = \rho$$

where $\vec{B}$ is magnetic induction, $\vec{H}$ – magnetic field, $\vec{D}$ – electric induction, $\vec{E}$ – electric field, ρ – volume charge density, $\vec{J}$ – current density, σ – electric conductivity of the medium.

The electric field in the time-domain is described by the following hyperbolic equation:

$$curl\,\mu^{-1}curl\,\vec{E} + \varepsilon\frac{\partial^2\vec{E}}{\partial t^2} + \sigma\frac{\partial\vec{E}}{\partial t} = -\frac{\partial\vec{J}}{\partial t},$$

where μ – magnetic permeability of the medium, ε - dielectric permittivity of the medium. We consider nonmagnetic media with $\mu = \mu_0, \varepsilon = \varepsilon_0$, hence, the displacement currents are negligible $\varepsilon\frac{\partial^2\vec{E}}{\partial t^2}$ in comparison to the conductive currents $\sigma\frac{\partial\vec{E}}{\partial t}$. As a result, we get the equation for the electric field in conductive medium:

$$curl\,\mu^{-1}curl\,\vec{E} + \sigma\frac{\partial\vec{E}}{\partial t} = -\frac{\partial\vec{J}}{\partial t}. \qquad (1)$$

We discretize the equation (1) with the vector finite element method. We introduce the following functional spaces:

$$H(grad,\Omega) = \{u \in L^2(\Omega) \mid \nabla u \in L^2(\Omega)\}$$
$$H(curl,\Omega) = \{\vec{u} \in L^2(\Omega) \mid \nabla\times\vec{u} \in L^2(\Omega)\} \quad ,$$
$$H_0(curl,\Omega) = \{\vec{u} \in H(curl,\Omega) \mid \vec{u}\times\vec{n}\big|_{\partial\Omega} = 0\}$$

with corresponding dot product and norm:

$$(\vec{u},\vec{v})_\Omega = \int_\Omega \vec{u}\cdot\vec{v}dx \quad \|\vec{u}\| = \sqrt{(\vec{u},\vec{u})_\Omega}$$
$$\|u\|^2_{H(grad,\Omega)} = \|u\|^2_\Omega + \|\nabla u\|^2_\Omega \quad \|\vec{u}\|^2_{H(curl,\Omega)} = \|\vec{u}\|^2_\Omega + \|\nabla\times\vec{u}\|^2_\Omega .$$

The variational formulation of the vector finite element method for the problem (1):

For $\vec{J} \in L^2(\Omega)\times(0,T)$ *find* $\vec{E} \in H_0(curl,\Omega)\times(0,T)$ *such that* $\forall\vec{W} \in H_0(curl,\Omega)\times(0,T)$:

$$\begin{aligned} &(\mu^{-1}curl\,\vec{E}, curl\vec{W})_\Omega + \sigma\left(\frac{\partial\vec{E}}{\partial t},\vec{W}\right)_\Omega = \\ &= -\left(\frac{\partial\vec{J}}{\partial t},\vec{W}\right)_\Omega - \int_{\partial\Omega}\mu^{-1}\left(\vec{W}\times\vec{n}\right)\cdot curl\vec{E}dS \end{aligned} \quad . \qquad (2)$$

The variational formulation (2) is discretized in the finite dimensional subspace of $H(curl,\Omega)$:

$$H^h(curl,\Omega) = span\left\{\vec{W}_1,\vec{W}_2,\ldots,\vec{W}_n\right\} \subset H_0(curl,\Omega) .$$

On the exterior boundary of the computational domain Ω, we set the following boundary conditions:

$$\vec{E}\times\vec{n}\big|_{\partial\Omega} = 0 .$$

The discretized variational formulation (2) is:

For $\vec{J} \in L^2(\Omega)\times(0,T)$ *find* $\vec{E}^h \in H^h(curl,\Omega)\times(0,T)$ *such that* $\forall\vec{W}^h \in H^h(curl,\Omega)\times(0,T)$ *:*

$$\begin{aligned} &(\mu^{-1}curl\,\vec{E}^h, curl\vec{W}^h)_\Omega + \sigma\left(\frac{\partial\vec{E}^h}{\partial t},\vec{W}^h\right)_\Omega = \\ &= -\left(\frac{\partial\vec{J}}{\partial t},\vec{W}^h\right)_\Omega \end{aligned} \quad . \qquad (4)$$

Taking into account expansion (3), we get the matrix form of the equation (4):

$$A\vec{e} + \sigma C\frac{\partial\vec{e}}{\partial t} = -\frac{\partial\vec{F}}{\partial t},$$

where

$$[A]_{ij} = \int_{\Omega} \mu^{-1} curl\vec{W}_i \cdot curl\vec{W}_j d\Omega, \quad i,j = 1, N_e$$
$$[C]_{ij} = \int_{\Omega} \vec{W}_i \cdot \vec{W}_j d\Omega, \quad i,j = 1, N_e \quad .$$
$$[F]_i = \int_{\Omega} \vec{J} \cdot \vec{W}_i d\Omega, \quad i = 1, N_e$$

To approximate problem (4) in time, we use an implicit three-level scheme with a varying time step [10]:

$$\begin{cases} A\vec{e}^n + C\dfrac{\vec{e}^n - \vec{e}^{n-1}}{\tau} = -\dfrac{\vec{F}^n - \vec{F}^{n-1}}{\tau}, \quad t \in (0, T_1) \\ A\vec{e}^n + \dfrac{\tau_2 + \tau_0}{\tau_2 \tau_0} C\vec{e}^n - \dfrac{\tau_2}{\tau_1 \tau_0} C\vec{e}^{n-1} + \dfrac{\tau_0}{\tau_1 \tau_2} C\vec{e}^{n-2} = 0, \; t \in (T_1, T_2) \end{cases} \quad ,(5)$$

where T_1 is the time of the current source disconnection, T_2 is the simulation end time, $\tau, \tau_0, \tau_1, \tau_2$ are the time-steps for regular and irregular time schemes.

Sufficiently small as the measurements begin, the time-step increases gradually to reach late measurement times in a small number of steps.

To simulate EMF signals, the software of numerical three-dimensional modeling ImpSoundV2 [9] was used, which implements the variational statement (4) with the time scheme (5)[10].

IV. Results

To identify the characteristic dependencies, we conduct a series of computational experiments. We analyze the results based on the anomalous EMF signals obtained as the relative difference between the EMF for models with an object and the EMF for half-space models in the receiver with the maximum EMF over the area. For a given probe setup, this is the central receiver with the number 25.

The first computational experiment is aimed at determining the dependence of signals on the depth of the upper edge of the object. Graphs of the anomalous EMF for models with different depths of the object are shown in Fig. 1. It can be seen that all EMF anomalies have a similar appearance. At early times, the curves decline to negative values until a minimum is reached, i.e. the EMF for the half-space model prevails over the EMF for the model with an object. Then the anomaly begins to increase until it reaches a certain maximum and decays to the EMF values of the half-space. This period is typical for the processes of filling the object with secondary currents and their attenuation to background values.

Fig. 1 shows that the moment of reaching the minimum of the EMF anomaly shifts with increasing depth of the upper edge of an object with a linear trend. Based on the obtained times of reaching the minimum, we can formulate the dependence of the depth of the upper edge on the time of reaching the minimum t_{min}:

$$h(t_{\min}) = 8.03 \cdot 10^6 \cdot t_{\min} - 7.89 \; .$$

This relationship is the first rough approximation for determining the depth of the upper edge of an object. Note that the maximum point also shifts when the object's depth changes, but the interval of increasing anomaly increases when it is deeper.

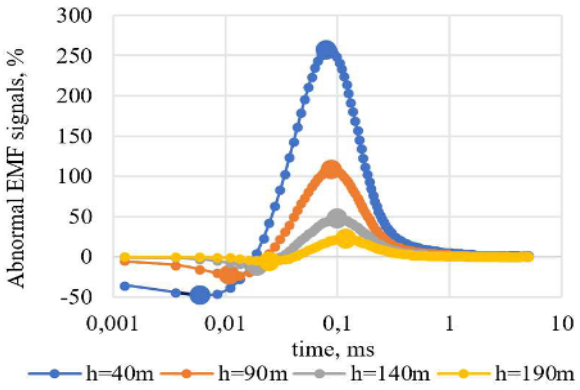

Fig. 1. Abnormal EMF signals for models with objects at depths of 40, 90, 140, and 190 m (on a logarithmic scale)

The next series of computational experiments is aimed at determining the generalized parameter of a conducting object– the induction mass. By induction mass we mean the product of the electrical conductivity of an object and its volume. Since the induction mass depends on two parameters, the following experiments are carried out:

- Fix the volume and change the electrical conductivity of the object
- Fix the electrical conductivity and change the volume

In all computational experiments, the depth of the object was recorded at the level of 40 m, and the resistance of the host medium was 1000 ohm·m to obtain the maximum amplitude of the signal anomaly.

Fig. 2 shows EMF anomalies for objects with different combinations of electrical conductivity and volume. The parameters of the considered objects are shown in Table 1. Object 1 has dimensions of 300x200x20 m. Objects 2 and 3 have dimensions of 300x200x10 m.

TABLE I. Parameters of Models

Object number	Induction mass, Cm/m^2	Volume, 10^3 m^3	Electrical conductivity, Cm/m
1	120 000	1200	0.1
2	120 000	600	0.2
3	60 000	600	0.1
4	60 000	600	0.1

Fig. 2 shows that at a fixed depth of occurrence, the anomaly minimum point has no displacement. The maximum point and maximum amplitude of the signal anomaly varies widely depending on the object's induction mass. Moreover, the interval of anomaly increase linearly depends on the growth of the induction mass. The anomaly's amplitude does not increase linearly. Fig. 2 shows that for a fixed induction mass (objects 1 and 2), the anomalous EMF signals have a similar character of increasing the anomaly, but a different amplitude of the anomaly maximum at comparable times of reaching the maximum. This leads to the following conclusions: abnormal EMF signals are complexly dependent on the object's induction mass; within a single induction mass, there is a variation in the distribution of EMF signals over the time of increase and the magnitude of the maximum anomaly. The electrical conductivity has a more significant effect on the anomaly amplitude than the

volume. The volume distribution in space has a significant

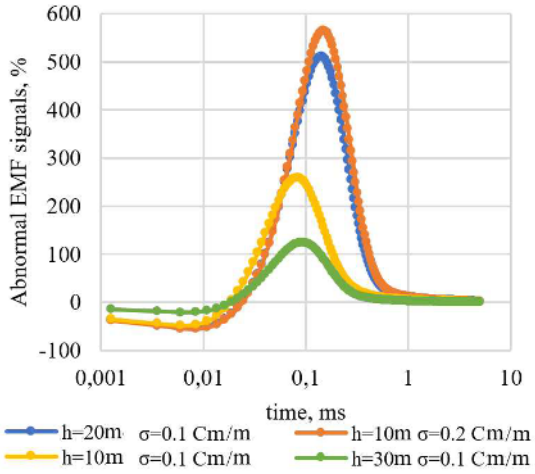

Fig. 2. Abnormal EMF signals for models with objects of different electrical conductivity and volume (on a logarithmic scale).

effect on the anomaly amplitude. Most likely, this is due to a change in the horizontal cross-sectional area of the object, on which the secondary current is induced when interacting with the primary field. The moment of the secondary current is proportional to the cross-sectional area and charges arising at the boundary of the object, depending on the resistances of the host medium and the object. If the cross-sectional area of the object is constant and its resistance changes, the value of the induced secondary current changes, which is also reflected in the change in the anomaly amplitude. However, the variations associated with the resistance are not as significant as the change in the area of the moment of secondary currents. The shift in the time of reaching the anomaly maxima for different object resistances can be related both to different initial moments of secondary currents and to different field propagation rates in the object.

Based on the assumption that the moment of secondary currents depends on the charges induced at the boundary, we conduct a series of computational experiments to estimate the influence of the host medium on the time of increase of the anomaly and its amplitude. The results of such experiments are shown in Fig. 3 and 4. Fig. 3 shows that when considering weakly conducting media with resistances from 500 to 1200 ohms·, the interval of anomaly increase practically does not change with increasing medium resistance. The electrical conductivity of the body has a significant effect. More conductive host media, for example with a resistance of 100 ohms·m, violate this dependence due to changes in the dynamics of the primary field propagation.

For a fixed object, the anomaly amplitude for different contrasts of the electrical conductivity of the body and the medium is shown in Fig. 4. We can observe a quadratic dependence of the maximum amplitude on the electrical conductivity of the body, and the coefficients of this dependence change with variations in the resistance of the host medium. Such a complex relationship can be expressed by the following formula:

$$A(\rho)=(0.001\cdot\rho^2+1.1343\cdot\rho-237.78)\cdot\sigma_{body}{}^2+$$
$$(0.0007\cdot\rho^2+1.8746\cdot\rho+78.42)\cdot\sigma_{body}+$$
$$+(-4\cdot10^{-5}\cdot\rho^2+0.023\cdot\rho-2.4243)$$

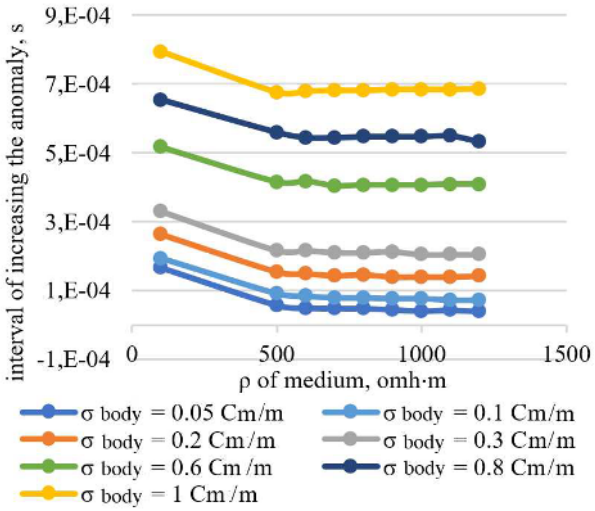

Fig. 3. Dependence of the interval of increasing the anomaly Δt on the values of the medium resistances ρ of the host medium for different electrical conductivities of ore objects

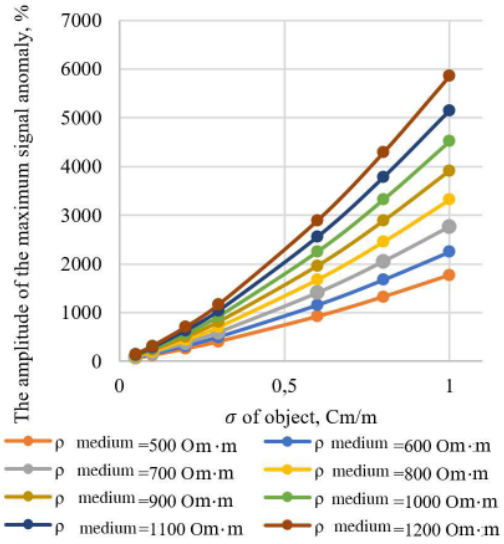

Fig. 4. Dependence of the amplitude of the maximum signal anomaly on the values of the specific electrical conductivity of an object σobject in weakly conducting media

This formula is quite accurate for the selected object. Table 2 shows the calculated estimates of the electrical conductivity of the object for the host medium of 700 ohm·m and the depth of 40 m.

TABLE II. ERROR ESTIMATES

True σ_{object}, Cm/m	Amplitude, %	Calculated σ_{object}, Cm/m	Error,%
0.05	85.55	0.0447	11.8
0.1	175.42	0.0926	7.99
0.2	373.25	0.1901	5.22
0.3	597.09	0.2902	3.38
0.6	1408.77	0.5953	0.79
0.8	2052.87	0.7972	0.35
1	2768.02	0.9953	0.47

Consider a more complex model of the environment. The previously considered layered object with dimensions of

300x200x10 m is covered by a near-surface layer with a resistance of 50 Ohm·m with a power of 40, 60 or 80 m. A layer that is more conductive than the host medium changes the behavior of the induced EMF curves, and the effect of the object manifests itself at a later time. Graphs of anomalous signals retain their characteristic appearance with a local minimum and maximum. Compared to the model of an object in half-space, the time to reach the anomaly minimum increases significantly. The shift in the time to reach the minimum for models with different thickness of the upper layer is proportional to the thickness of the layer, i.e. the difference between models with an overlapping layer with a thickness of 40 and 80 m is almost two times (Fig. 5). Fig. 5 shows that the dependence of anomalous signals of the object's influence on the EMF relative to the EMF of a layered model without an object is similar to the dependence of anomalies on an object in half-space. However, the previously obtained dependencies should be adjusted to account for the influence of the upper overlapping layer. The time to reach the anomaly minimum for a model with an overlapping layer depends not only on the distance to the object, but also on the parameters of the upper layer. The anomaly amplitude decreases significantly as the thickness of the overlapping layer increases. With a layer thickness of 80 m, the amplitude of the anomalous signal does not exceed 8%, which is close to the limit of sensitivity of measuring devices.

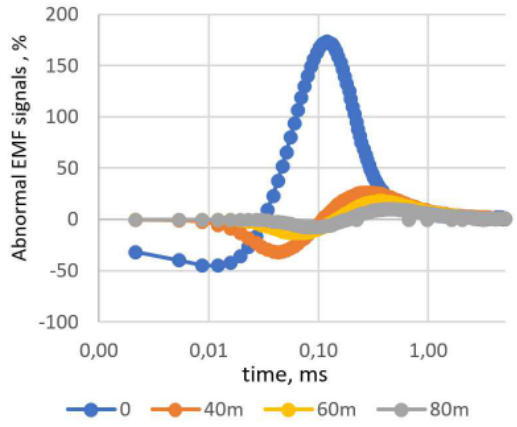

Fig. 5. Abnormal EMF signals for models with an object covered by a layer of different power (on a logarithmic scale).

V. Conclusions

In this paper, numerical three-dimensional modeling of the electric field and EMF signals from a conducting layer-like body in a weakly conducting space is performed. Analysis of anomalous EMF signals obtained when comparing signals from a model with an object in relation to a model without an object showed that it is possible to estimate the depth of the upper edge of the target object and its induction mass (the product of the object's electrical conductivity by its volume) from measurements of EMF signal anomalies without using three-dimensional inversion procedures. The revealed dependences of the time of signal anomaly increase on the depth of the upper edge are quite stable. The dependence of the maximum amplitude of the signal anomaly obtained for a specific object can be corrected for use on objects with a similar induction mass, but a different moment of secondary currents. For objects covered by a conducting layer, the distribution of anomalies over time is preserved, but the dependencies need to be adjusted to take into account the time required for field propagation in the upper layer.

Acknowledgment

The research was supported by RSF (project No. 25-71-10045) High-performance algorithms of multiscale numerical modeling for solving applied problems of exploration geophysics in the northern regions of Russia.

References

[1] V. I.Dmitriev, Inverse problems of electromagnetic sounding, (in Russian). Moscow, Nauka Publ., 2005

[2] M. V.Berdichevsky, V. I. Dmitriev, Mathematical problems of electrical exploration, (in Russian). Moscow, Nauka Publ., 2009

[3] G. Anger, R. Gorenflo, H. Jochmann, H. Moritz and W. Webers, Inverse Problems: Principles and Applications in Geophysics. Akademie Verlag, Berlin, 1993.

[4] K. Bauer, G.Munoz, I. Moeck, “Pattern recognition and lithological interpretation of collocated seismic and magnetotelluric models using self-organizing maps,” Geophysical Journal International, vol.189, pp.984-998, 2012, doi: 10.1111/j.1365-246X.2012.05402.x.

[5] G. E. Backus, “Bayesian inference in geomagnetism,” Geophysical Journal International, vol. 92, is. 1, pp. 125–142, 1988, doi: 10.1111/j.1365-246X.1988.tb01127.x

[6] V.V.Spichak, Computational Geo-Electromagnetics: Methods, Models, Forecasts. Elsevier, Cambridge, USA. 2020

[7] V.Spichak, “Modern Methods for Joint Analysis and Inversion of Geophysical Data,” Russian Geology and Geophysics. vol. 61, pp. 341-357, 2020, doi:10.15372/RGG2019092.

[8] M.Shimelevich, E. Rodionov, I. Obornev, E. Obornev, “Application of Convolutional Neural Networks in Inverse Problems of Geoelectrics,” Izvestiya, Physics of the Solid Earth, vol. 60, pp. 1215-1227, 2025, doi: 10.1134/S1069351324701039

[9] N. V. Stabel, “Computer program ImpSoundV2”, Certificate of state registration of computer program No. 2020665691, 2020

[10] N. V. Shtabel, M. I. Epov, E. Antonov, M. A. Korsakov “Approximation of a near-vertical boundary in the problems of pulsed electromagnetic soundings”, Russian Geology and Geophysics, vol. 55, no. 1, pp. 89-97, 2014, doi:10.1016/j.rgg.2013.12.007